

The adsorption of water on clean and oxygen predosed Rh(111): Surface templating via (1×1)-O/Rh(111) induces formation of a novel high-density interfacial ice structure

K. D. Gibson, M. Viste, and S. J. Sibener^{a)}

*The James Franck Institute and The Department of Chemistry, The University of Chicago,
5640 South Ellis Avenue, Chicago, Illinois 60637*

(Received 13 August 1999; accepted 16 February 2000)

Water adsorbed on clean Rh(111) forms an ordered structure with a $(\sqrt{3}\times\sqrt{3})R30^\circ$ diffraction pattern. This is facilitated by the close match of surface lattice constants for Rh(111) and the (0001) face of hexagonal ice, I_h . The preadsorption of small quantities of disordered oxygen improves the long-range ordering of the water overlayer. When a well-ordered half-monolayer of oxygen is grown on the Rh(111) prior to H₂O exposure, there is no evidence of any long-range ordering of the water. However, when H₂O is adsorbed on a (1×1)-O/Rh(111) surface, where there is a well-ordered monolayer of adsorbed oxygen, the adsorbed H₂O forms a new high-density structure exhibiting a (1×1) diffraction pattern. The adsorbed H₂O structure is epitaxial with respect to the underlying oxygen and rhodium. This structure persists for many layers of adsorbed water. On the clean Rh(111) surface, water molecules are adsorbed through the oxygen lone pair orbital. When the surface is fully covered with oxygen, the first layer of water can hydrogen bond to the surface, i.e., they likely adsorb with one or both of the hydrogen atoms pointing toward the surface. This creates a template for a novel structure that forms at low pressure, producing a high-density crystalline form of interfacial ice. This discovery suggests that other molecules, especially those that hydrogen bond, may form new structures on metals covered with a high-density oxygen overlayer, with associated consequences for interfacial chemistry. © 2000 American Institute of Physics. [S0021-9606(00)70118-8]

INTRODUCTION

Studying the adsorption of H₂O on metal surfaces is important because of its role in catalysis, corrosion, and electrochemical reactions. Ice grown on Ru(0001) has even been used for understanding the chemistry and physics of atmospheric ice crystals.¹ Under the conditions at which these processes normally occur, the metal surface may be modified by the adsorption of other species, oxygen certainly being one of the more ubiquitous. Studying these systems under ultrahigh vacuum (UHV) conditions allows for the careful control of the surface structure and composition, and characterization utilizing surface-sensitive techniques that are not available at higher pressures. In this paper, we report the results of experiments detailing the adsorption of H₂O on clean and O-covered Rh(111). The techniques used were temperature-programmed thermal desorption (TPD) and the scattering of a supersonic He beam. TPD spectra give information on relative surface coverages as well as information on the energetics of the adsorbate-surface interactions. The diffraction of He atoms is a technique to obtain structural information that is exclusively surface sensitive, nondestructive, and can be easily used with insulating adsorbates.

Most of the previous studies of the ordered adsorption of water on the atomically smooth faces of transition metal surfaces under UHV conditions have used either Pt²⁻⁶ or

Ru.^{1,7-16} Only a few have used Rh.¹⁷⁻¹⁹ There is a somewhat dated but quite extensive review of water adsorption on solid surfaces.²⁰ On Ru(0001), it is possible to grow ordered layers of ice epitaxially. The structure is that of hexagonal ice, I_h , with the (0001) face exposed to the vacuum. This gives a $(\sqrt{3}\times\sqrt{3})R30^\circ$ diffraction pattern; the formation of this ordered overlayer is facilitated by the close match between lattice constants: 4.50 Å for the a lattice constant of bulk hexagonal ice,²¹ I_h , near 100 K and 4.68 Å for Ru(0001). Rh(111) actually has a slightly more favorable lattice constant, the $(\sqrt{3}\times\sqrt{3})R30^\circ$ dimension being 4.66 Å. On both surfaces, water is adsorbed molecularly.

With this similarity, and their proximity in the periodic table, the growth of physisorbed H₂O overlayers should be closely analogous for Ru(0001) and Rh(111). On Ru(0001) the completed layer closest to the metal surface is called a bilayer (BL) because the oxygen atoms lie on two different planes.⁷⁻¹⁶ The ideal coverage would be 0.67 monolayers (ML) (1 ML=1.6×10¹⁵/cm²). In this paper, whenever we refer to a bilayer, it is in reference to this $(\sqrt{3}\times\sqrt{3})R30^\circ$ structure. The actual coverage has been measured to be ~0.6,⁹ but there is reason to believe that the adsorbed H₂O forms a striped phase with regions of bare Ru between ordered domains of H₂O.^{12,13} Interestingly, this ordered layer gives two distinct peaks in thermal desorption spectra, their ratios dependent upon the heating rate. Further adsorbed H₂O forms multilayer ice that desorbs at a lower temperature than the first bilayer.

^{a)}Author to whom correspondence should be addressed. Electronic mail: s-sibener@uchicago.edu

The Rh(111) surface behaves similarly. The thermal desorption spectra show distinct desorption features: the lowest-temperature feature we assign to multilayer ice, and the higher-temperature feature(s) to the bilayer. Both the bilayer and multilayer exhibit long-range order in the form of a $(\sqrt{3}\times\sqrt{3})R30^\circ$ diffraction pattern.

Preadsorbing oxygen on transition metal surfaces, whether ordered or disordered, often disrupts the long-range ordering of adsorbed H_2O .^{10,22} These studies were done with less than a full monolayer of oxygen. We found that there was no long-range ordering of adsorbed water when growth was attempted on a previously deposited well-ordered half-monolayer of oxygen on Rh(111). Using an O atom beam, we have been able to adsorb a well-ordered full monolayer of oxygen on Rh(111).^{23,24} When this surface is exposed to H_2O , a new overlayer structure for the adsorbed water is observed, giving a (1×1) diffraction pattern that persists up to several layers. On the clean Rh surface, the water adsorbs through the oxygen lone pair orbital. When the surface is fully covered with oxygen, the interaction is most likely between one or both of the hydrogen atoms of the water molecule and the preadsorbed oxygen. This provides a template for growing an entirely different form of crystalline ice than normally occurs.

EXPERIMENT

Only essential features of the scattering machine will be mentioned; further descriptions can be found elsewhere.^{23,25,26} We generate three simultaneous molecular beams that converge on the target crystal in the UHV scattering chamber. The differentially pumped quadrupole mass spectrometer (angular resolution of $\sim 1^\circ$) rotates around the position of the crystal. This rotation defines the plane in which we can detect scattered atoms.

Oxygen was deposited on the sample in two ways. For growing a half-monolayer $(2\times 1)\text{-O/Rh}(111)$, a beam of neat O_2 was expanded through a room temperature nozzle. For growing 1 monolayer $(1\times 1)\text{-O/Rh}(111)$, we passed neat O_2 through a radio-frequency discharge nozzle beam source, producing $\sim 30\%$ O atoms. The beam was supersonic but energetically broad, with the O_2 fraction having an average energy of $\sim 80\text{--}90$ meV, and the O fraction having an average energy of ~ 60 meV. For growing the ice overlayers, we made a beam of H_2O entrained in He by bubbling He (Linco, ultrahigh purity grade) through a stainless steel container of room temperature H_2O (Fisher, HPLC grade). The only treatment done was several cycles of pumping out the H_2O -filled bubbler and then purging with He. The expansion was through a 50 or 100 μ nozzle, and the H_2O flux, estimated at a few hundredths of a monolayer/s, was controlled by the backing pressure.

The rhodium crystal was cut to within 1° of the (111) face, as confirmed by Laue x-ray back-reflection spectroscopy. It was cryogenically cooled with either liquid N_2 or He and could be resistively heated to 1300 K. Crystal cleanliness was confirmed by Auger electron spectroscopy, and by monitoring the intensity and width of specularly reflected He. C could be removed by exposing the surface to O_2 at a

surface temperature $T_s=900$ K. Adsorbed oxygen was removed by heating the crystal to about 1250–1300 K for 3 min.

For the diffraction measurements, a liquid N_2 cooled nozzle beam source produced a highly collimated and essentially monoenergetic He beam [$\langle E \rangle \cong 20$ meV and a $\Delta v(\text{FWHM})/v \cong 1\%$]. Coverage measurements were done using temperature-programmed desorption, where the signal of desorbing molecules was monitored while the temperature of the crystal was ramped. For the $(\sqrt{3}\times\sqrt{3})R30^\circ$ structures grown on clean Rh(111), the coverage is given in terms of bilayers, where 1 BL is the first adsorption layer of H_2O , as discussed in the Introduction. In terms of absolute coverage, 1 BL = $1.07 \times 10^{15}/\text{cm}^2$. For overlayers grown on the $(1\times 1)\text{-O}$ covered Rh(111), the coverage is given in terms of a conventional monolayer, 1 ML = $1.6 \times 10^{15}/\text{cm}^2$.

RESULTS AND DISCUSSION

Water adsorption on Rh(111)

Bilayer H_2O

Structure. Figure 1 shows diffraction spectra for 1 BL of H_2O along two principal symmetry directions of Rh(111). The diffraction spectra are consistent with a $(\sqrt{3}\times\sqrt{3})R30^\circ$ overlayer structure, with a lattice constant of 4.64 ± 0.02 Å, larger than the 4.50 Å for the a lattice constant of bulk I_h .²¹ The peaks are narrow, indicating good long-range order, though there is evidence of small features near the specular, possibly suggesting a larger superlattice periodicity. To grow these overlayers, the surface was exposed to the $\text{H}_2\text{O/He}$ beam for at least 30 s with the surface temperature held at 160 K; the beam was then blocked and the sample immediately cooled. TPD spectra showed that continued dosing at this surface temperature led to no further H_2O adsorption. Consistent with the adsorption of H_2O on other surfaces, we assume that this represents one bilayer of adsorbed water.

Figure 2 shows further diffraction spectra and the corresponding TPD spectra. These spectra were taken on consecutive days, using the same $\text{H}_2\text{O/He}$ beam and the same crystal preparation. Yet, there are very clear differences in the quality of the overlayers. The He diffraction spectrum shown in Fig. 2(a) is more intense than that in Fig. 2(c), and shows almost no hint of any added features near the specular. The spectrum in Fig. 2(c) shows quite distinct peaks near the specular, in this case indicating a superlattice structure with a repeat distance of ~ 24 Å. (Though always present, the positions and intensities were not fully reproducible, being quite sensitive to sample preparation.) The TPD spectra both have a large peak with a maximum desorption intensity at 170 K, but the better-ordered overlayer has a further high-temperature peak at ~ 200 K. Throughout the duration of these experiments, we grew overlayers that had diffraction spectra similar to that shown in Fig. 2(a) and others similar to Fig. 2(c). The better ordered overlayers always showed a high-temperature feature in the TPD spectrum.

Previous work on Rh(111) surfaces show a desorption peak for low H_2O coverages between 180 and 190 K.^{17–19} As further H_2O is adsorbed, a low-temperature peak at ~ 160 K grows in. The high-temperature peak is ascribed to the first

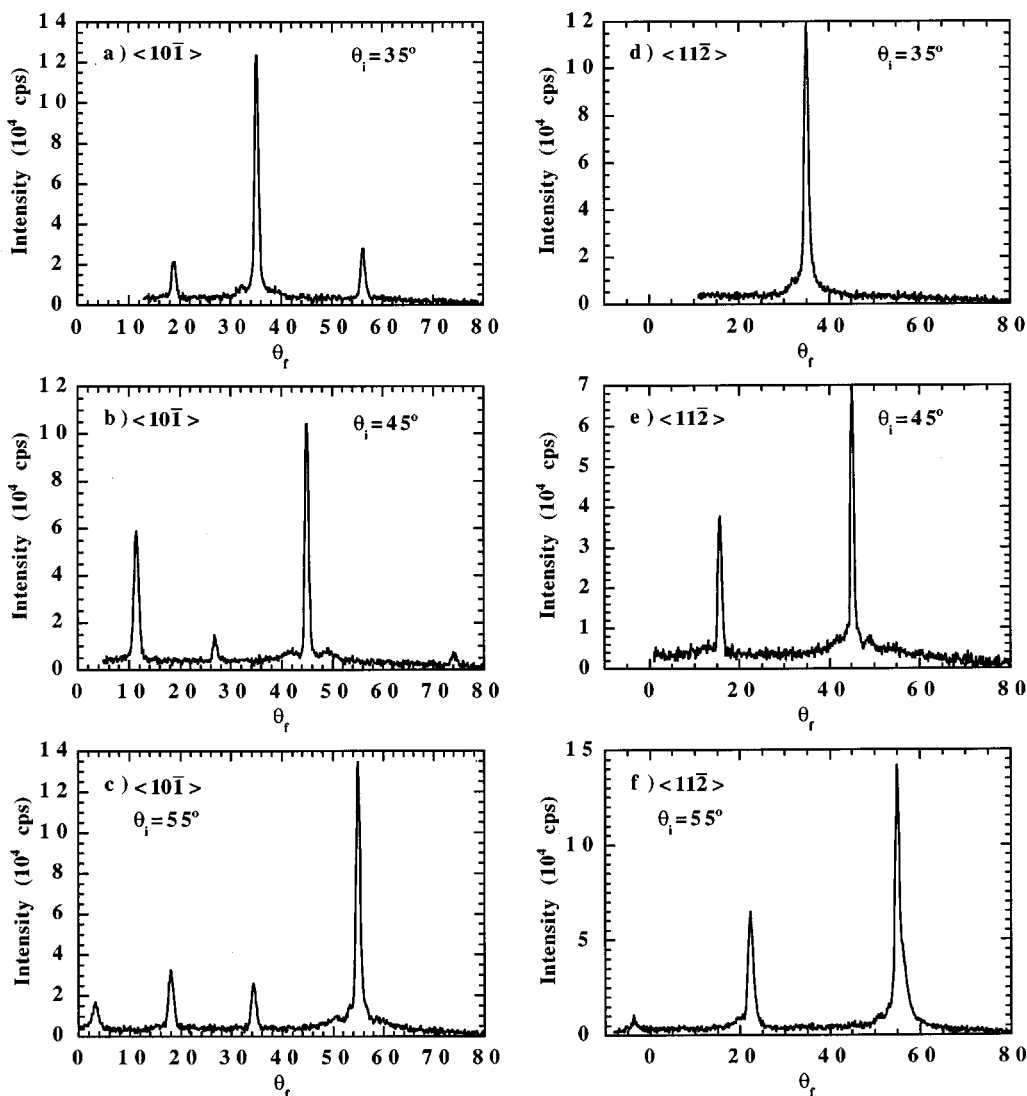


FIG. 1. He diffraction spectra of 1 BL H₂O Rh(111) taken along two principal symmetry directions and at three different incident angles, with $E_i = 19.9$ meV and $T_s = 80$ K. There was ~ 0.02 ML of adsorbed oxygen, estimated from the TPD spectrum.

bilayer, and the low-temperature peak to a thicker overlayer. Both Kiss and Solymosi¹⁷ and Wagner and Moylan¹⁸ saw a long tail on the high-temperature side of the low coverage desorption feature, but no resolved peak at a higher temperature. Wagner and Moylan found that if even a small amount of oxygen is adsorbed onto the surface before H₂O exposure, the TPD spectra develop an additional feature between 210 and 215 K. Zinck and Weinberg¹⁹ saw an additional feature at ~ 220 K, but they also saw the feature due to a thin multilayer move up by ~ 10 K, something that we did not observe. The results of Wagner and Moylan suggest that, in the presence of oxygen, some of the water dissociates to form adsorbed hydroxyls. The high-temperature TPD peak is due to the disproportionation of these hydroxyls and the desorption of some closely associated intact water molecules.

Our experiments indicate that the better-ordered overlayers are due to a small amount of some coadsorbate, quite possibly oxygen; they occurred with a slower cool-down after cleaning the crystal, allowing a longer time for the adsorption of background gases. Oxygen is one possibility; when the surface was exposed to the O₂ beam at very low

fluxes and for a short time at $T_s = 325$ K, the diffraction spectra got much more intense, and the TPD spectra showed sizable high-temperature shoulders.

To quantify this effect, we calibrated the oxygen coverage by observing the attenuation of specular He scattering.²⁷ For low coverages, this showed a power law dependence consistent with disordered adsorption. We were able to estimate the coverage as a function of specular scattering attenuation,

$$\frac{I}{I_0} = (1 - m\Theta_0) \sum_A n_s / m, \quad (1)$$

where I_0 is the specular intensity before O₂ exposure, I is the intensity after, n_s is the reciprocal of the unit cell area, 0.16 \AA^{-2} for Rh(111), and $m = 2$ since the saturation coverage for O₂ dosing is 0.5 ML. The fitted value derived for the cross section, \sum_A , is 179 \AA^2 . This is large but not unreasonable.

With this information, we adsorbed small, known quantities of oxygen at $T_s = 325$ K on the clean Rh surface. We used LHe cooling so that the surface cooled quickly and

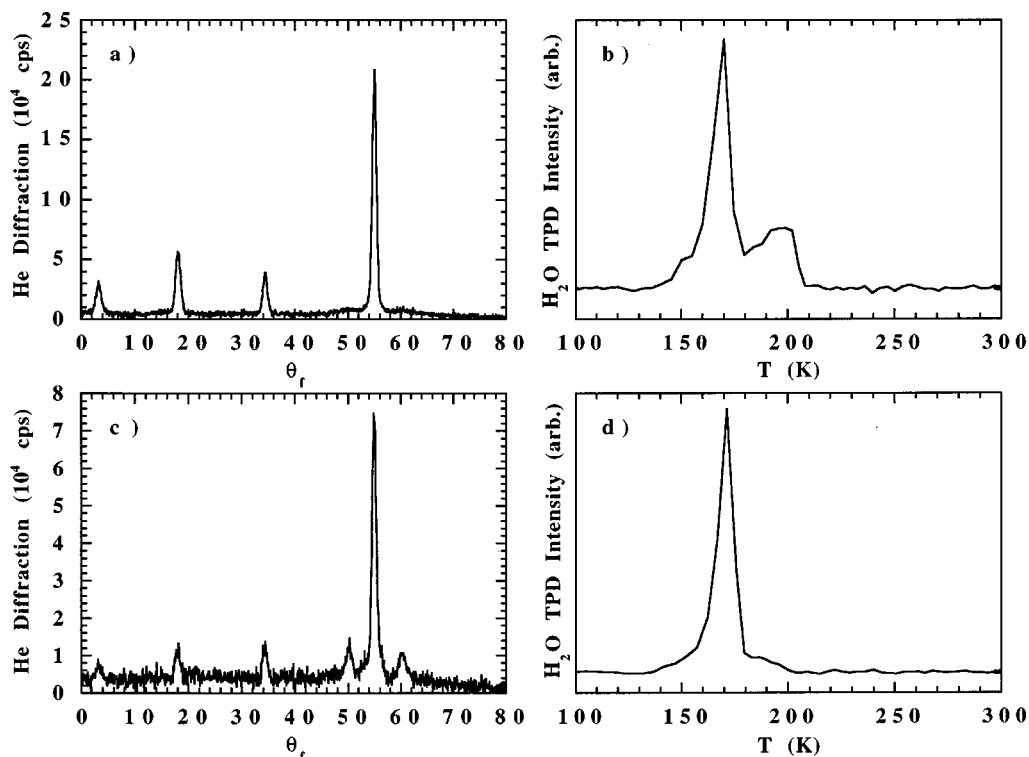


FIG. 2. He diffraction spectra taken along the $\langle 10\bar{1} \rangle$ azimuth at $\theta_i = 55^\circ$ and with $E_i = 19.8$ meV for two different $\text{H}_2\text{O}/\text{Rh}(111)$ surfaces. $T_s = 100$ K for the spectrum in (a) and 80 K for the spectrum in (c). (b) is the H_2O TPD spectrum for the overlayer whose diffraction spectrum is shown in (a) and (d) is the H_2O TPD spectrum for the overlayer whose diffraction spectrum is shown in (c). The TPD spectra were taken with a ramp rate of 200 K/min.

remained as clean as possible. The crystal was then cooled to 160 K before adsorbing 1 BL of H_2O . When the coverage of preadsorbed oxygen was less than <0.01 ML, there was no significant improvement in the diffraction spectra. However, for coverages between about 0.02 and 0.05 ML, the diffraction spectra became quite intense, with narrow features and, at most, small shoulders on the sides of the expected diffraction features. As was also observed by Wagner and Moylan,¹⁸ the relative size of the high-temperature H_2O desorption peak is directly related to the oxygen coverage for low coverages. The ratio of this peak to the total area of the BL desorption peak as a function of oxygen coverage can be calibrated against the previous procedures. Using this calibration, the overlayer that yielded the spectra in Figs. 2(a) and 2(b) had about 0.02 ML of adsorbed oxygen.

The important points here are that the H_2O overlayers we grew on Rh(111) always showed a diffraction pattern consistent with a $(\sqrt{3} \times \sqrt{3})R30^\circ$ structure for the adsorbed water, and within our reproducibility, the amount of adsorbed H_2O was the same whether the TPD spectra showed one peak or two. Small amounts of preadsorbed oxygen resulted in a vast improvement in the long-range order of the H_2O overlayer, but had no effect on the basic structure.

Debye–Waller analysis. The amplitudes of the perpendicular motion of the adsorbate can be estimated by measuring the Debye–Waller factor,

$$I = I_0 \exp(-4k_z^2 \langle u_z^2 \rangle), \quad (2)$$

where I is the reflected He intensity and $\langle u_z^2 \rangle$ is the mean-

squared displacement of the surface atoms. The perpendicular momentum of the He, k_z , includes the He-surface well-depth, D :

$$\frac{\hbar^2 k_z^2}{2M_{\text{He}}} = (E \cos^2 \theta_i + D), \quad (3)$$

where M_{He} is the He mass and E_i the incident energy. The measurement is accomplished by monitoring the specular intensity as a function of surface temperature and incident angle. The rms (root-mean-squared) amplitude can be estimated by a simple Debye model,²⁸

$$\langle u_z^2 \rangle = \frac{3\hbar^2 T_s^2}{M_s k_B \Theta_D^3} \int_0^{\Theta_D/T} y \coth(y) dy, \quad (4)$$

where k_B is the Boltzmann constant, Θ_D is the surface Debye temperature, and M_s is the mass of an adsorbed H_2O . The result is that $\Theta_D = 300 \pm 70$ K, using a best-fit well depth of 4 meV, compared with a Debye temperature for bulk ice I_h of ~ 220 K.^{29,30} The large error bar is at least partially due to the narrow temperature range we could use, 80–140 K.

Multilayer H_2O

Structure. Figure 3 shows diffraction spectra for 24 BL $\text{H}_2\text{O}/\text{Rh}(111)$, taken along the $\langle 10\bar{1} \rangle$ azimuth. As the number of layers increases, the diffraction intensities get progressively attenuated, but with even this thick overlayer, there are still clear diffraction peaks; the $(\sqrt{3} \times \sqrt{3})R30^\circ$ structure persists, and the lattice constant is 4.64 ± 0.02 Å. The H_2O

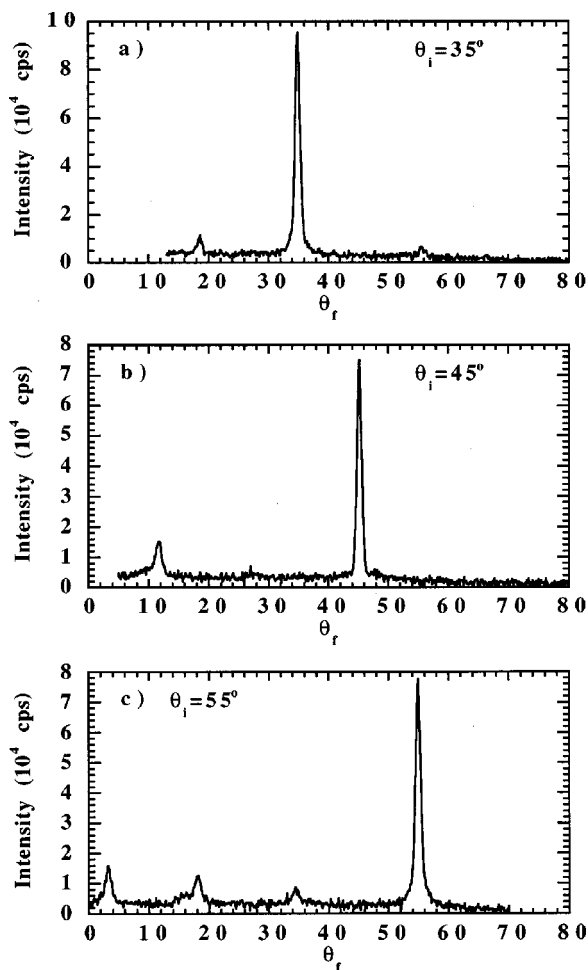


FIG. 3. He diffraction spectra of 24 BL $\text{H}_2\text{O}/\text{Rh}(111)$ taken along the $\langle 10\bar{1} \rangle$ direction and at three different incident angles, with $E_i = 19.9$ meV and $T_s = 80$ K.

overlayer was grown by dosing at $T_s = 160$ K for 40 s, and then cooling to 145 K while dosing was continued for another 10 min. This was the highest temperature we could use and still grow multilayers in a reasonable amount of time, and was high enough to grow crystalline rather than amorphous ice.³¹ The first part of the dosing procedure grows a well-ordered bilayer, and was critical for growing well-ordered multilayers; the quality of the multilayer was highly dependent on the quality of the bilayer on which it was grown. The additional adsorbed H_2O resulted in a low-temperature peak in the TPD spectra, similar to that seen with other transition metal surfaces. This is shown in Fig. 4, for quantities of adsorbed H_2O slightly greater than 1 BL. Again, the better-diffracting surface shows an extra feature in the TPD spectrum at ~ 200 K.

One issue our experiments have not addressed is the exact chemical nature of the ice surfaces, i.e., the precise geometry of the surface hydroxyl groups has not been ascertained. It would be reasonable to expect that the normally proposed structure of the ice bilayer on transition metals would cause subsequent layers to be adsorbed in such a way that the surface would be composed of dangling OH groups. The recent calculations of Witek and Buch³² show that even for only a few layers, the structure is modified in such a way

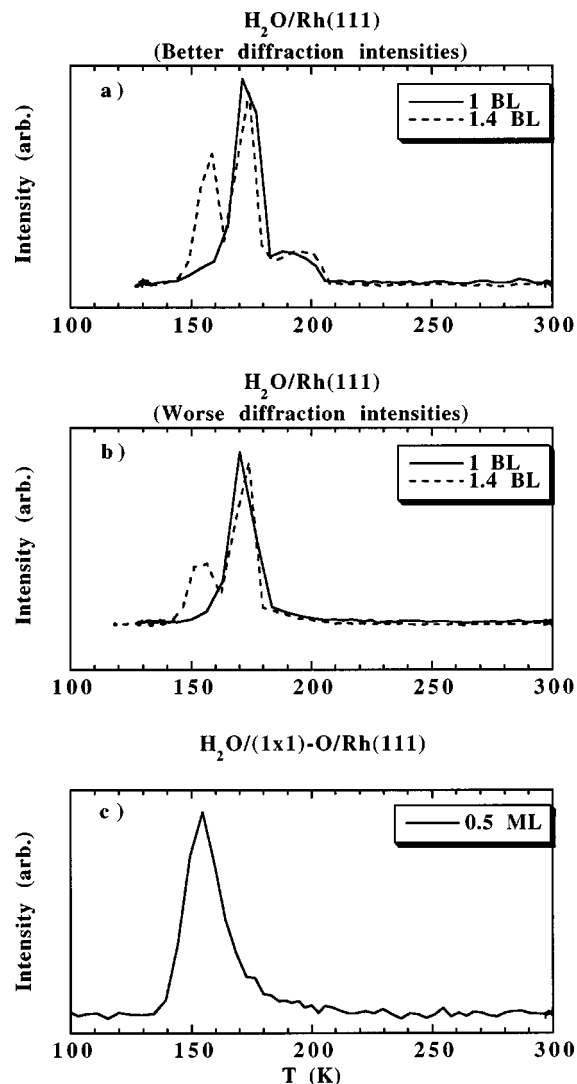


FIG. 4. Examples of H_2O TPD spectra for different H_2O covered surfaces. The ramp rates were 200 K/min.

that there are few dangling hydroxyls at the surface. The experiments of Schaff and Roberts³³ show evidence that there are few, if any, such groups on the surface of thin crystalline ice films, and demonstrate that this has a profound influence on the surface chemistry.

Debye-Waller analysis. For the adsorption of multilayers of H_2O on $\text{Pt}(111)$, it has been suggested that the outermost water molecules have a very large vibrational amplitude; a rms amplitude perpendicular to the surface of at least 0.25 Å at 90 K.^{4,5} The observed intensities of the diffraction features make such a large motion unlikely in the case of overlayers grown on Rh. A rms amplitude of 0.25 Å at 90 K corresponds to a surface Debye temperature of 115 K using the previously mentioned model, implying a specular attenuation at $\theta_i = 45^\circ$ of $I = 10^{-3} I_0$. This would make the diffraction very weak. By comparison, with a Debye temperature of 300 K, the intensity would still be $\sim 20\%$ of I_0 . For the narrow range of temperatures we had, it was difficult to extract a precise number. However, with a surface Debye temperature of 115 K, the specular intensity at $\theta_i = 45^\circ$ would decrease by a factor of 30 in going from a surface tempera-

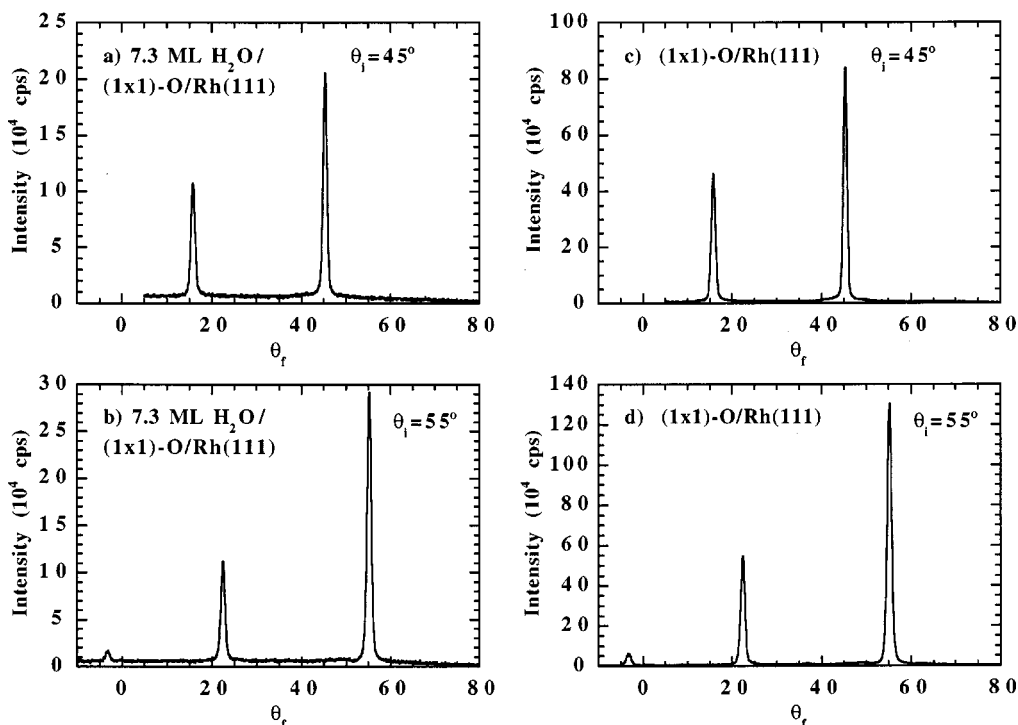


FIG. 5. He diffraction spectra taken along the $\langle \bar{1}2\bar{1} \rangle$ azimuth with $E_i = 19.8$ meV and $T_s = 120$ K. (a) and (b) are for 7.3 ML H_2O grown on the (1 \times 1)-O overlayer whose spectra are shown in (c) and (d).

ture of 70 to 130 K, the temperature range of our experiments. *The observed change was less than a factor of 2*, close to that of a bilayer of adsorbed water. Using a $\Theta_D = 300$ K, the rms vibrational amplitude is ~ 0.12 Å at $T_s = 90$ K. In summary, the relatively intense diffraction features, coupled with their insensitivity to surface temperature, means that the vibrational amplitude of the top layer of water is *much* smaller than was estimated for ice on Pt(111) by Materer *et al.*^{4,5} A more recent He scattering study of multilayer ice adsorbed on Pt(111) estimated a surface Debye temperature of 175 K,⁶ a significantly higher value, but still probably less than for water adsorbed on Rh(111).

Water adsorption on ordered oxygen/Rh(111)

Half-monolayer (2 \times 1)-O

In earlier papers, we discussed the adsorption of a half- and full monolayer of oxygen on the Rh(111) surface.^{23,24} We will now examine the structure of adsorbed H_2O on these modified Rh surfaces. First, a surface with a well-ordered half-monolayer of adsorbed oxygen was prepared. The H_2O dosing procedures were the same as that used for the clean Rh surface, but there were no diffraction features other than a weak specular peak on a large incoherent background. The TPD spectra for an amount of adsorbed H_2O equivalent to 1 BL looked similar to the spectrum in Fig. 2(b), and larger amounts of adsorbed H_2O had a spectrum like that shown in Fig. 4(a), they both showed a distinct feature at ~ 200 K. After the H_2O had been desorbed, the oxygen-covered surface still had the same diffraction pattern. That the TPD spectra are similar suggests that the bonding of H_2O is similar on both the nearly clean and oxygen covered surface, but the lack of distinct features in the diffraction spectra indi-

cates that a half-monolayer of oxygen prevents any long-range ordering in the H_2O overlayer. This is the same result as for both Ni(111)²² and Ru(0001),¹⁰ where the preadsorption of any amount of oxygen interferes with the long-range ordering of adsorbed H_2O . Based on HREELS measurements for a saturation coverage of O/Ru(0001), Thiel *et al.*¹⁵ thought that there might be some long-range ordering of the water at elevated temperatures, but Doering and Madey¹⁰ found no evidence of this with LEED.

Full monolayer (1 \times 1)-O

In contrast, Figs. 5 and 6 show diffraction spectra for H_2O adsorbed on a (1 \times 1)-O/Rh(111) surface along two principle symmetry directions. The H_2O overlayer was grown by exposing the (1 \times 1)-O/Rh(111) surface to a low flux H_2O /He beam at $T_s = 140$ K. Also shown are the corresponding diffraction spectra of the oxygen-covered surface before the H_2O was adsorbed. The (1 \times 1) diffraction pattern is retained, and the lattice constant of 2.68 ± 0.01 Å is the same. The principal difference is an attenuation of the coherent signal. How rapidly the diffraction features are attenuated with increasing H_2O coverage is dependent on both the flux and the surface temperature, with the best overlayers grown with the lowest flux and the highest surface temperatures. We have grown a diffracting overlayer having 20 ML of H_2O by dosing for 45 min at $T_s = 140$ K. The spectra show no hint of the $(\sqrt{3} \times \sqrt{3})R30^\circ$ structure expected for the surface of ice I_h . [As discussed in the experimental section, we give the coverage in terms of a conventional monolayer (1 ML = $1.6 \times 10^{15}/\text{cm}^2$) for the water structures grown on (1 \times 1)-O. The term bilayer (BL) refers to the first adsorption layer of

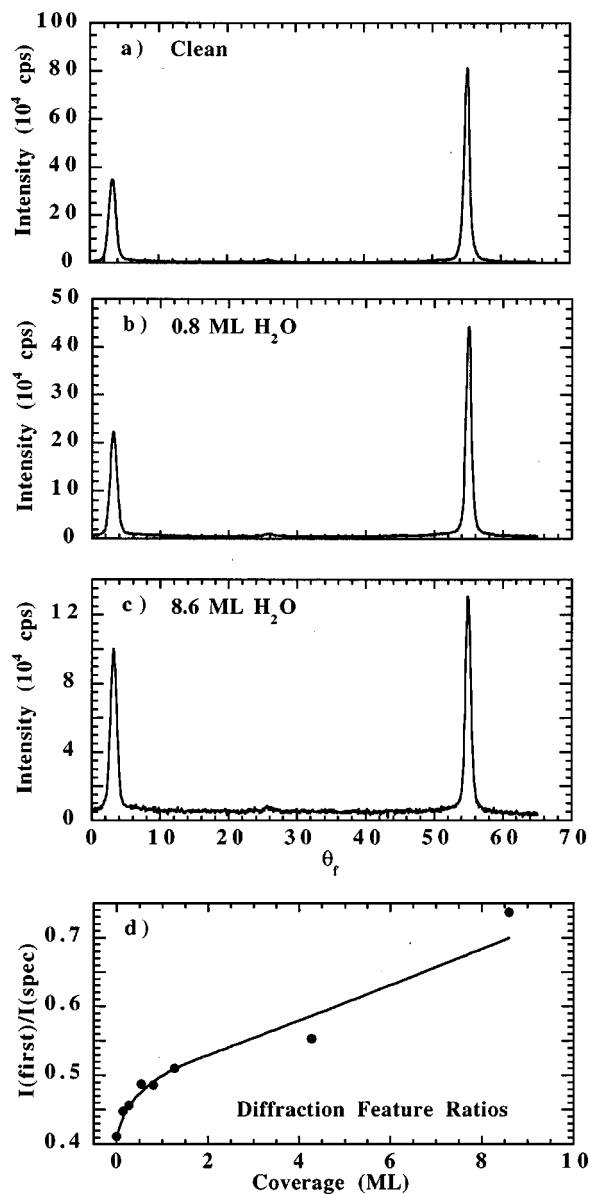


FIG. 6. (a)–(c) show He diffraction spectra taken along the $\langle 01\bar{1} \rangle$ azimuth at $\theta_i = 55^\circ$, and with $E_i = 19.8$ meV and $T_s = 120$ K, for varying amounts of H₂O adsorbed on a (1×1) -O/Rh(111) surface. (d) is a plot of the ratio of the first-order diffraction peak near normal and the specular peak at $\theta_f = 55^\circ$ as a function of H₂O coverage. Points are the experimental data, while the line is drawn to guide the eye.

the $(\sqrt{3} \times \sqrt{3})R30^\circ$ structure of H₂O adsorbed on Rh(111). By this convention, $1 \text{ BL} = 0.67 \text{ ML} = 1.07 \times 10^{15} / \text{cm}^2$.]

A TPD spectrum is shown in Fig. 4(c). The position of the maximum desorption rate is essentially identical to that for the multilayer feature from H₂O adsorbed on the clean Rh(111) surface. No more distinct features occur in the spectrum as further H₂O is adsorbed on the (1×1) -O/Rh(111) surface.

Since the positions of the diffraction features are the same before and after exposure to water, the question arises as to whether the H₂O is wetting the surface. One possibility is that the water is forming incoherently scattering islands, and the observed diffraction is from regions of bare (1×1) -O. Figures 6(a)–(c) show in more detail what happens

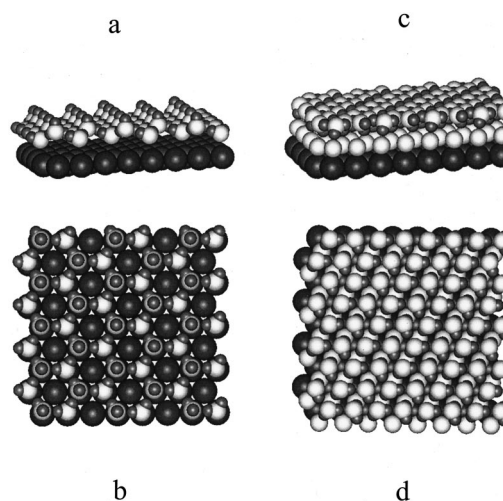


FIG. 7. Panels (a) and (b) show proposed side and top views of the bilayer structure for water adsorbed on Rh(111), identical with the known structure on Ru(0001) (Refs. 10, 20, and 35). Panels (c) and (d) show side and top schematic views of the proposed structure for water adsorbed on monolayer oxygen. Note that the density and orientation of the water molecules in the two structures differ markedly.

as progressively more H₂O is adsorbed on the (1×1) -O/Rh(111) surface. The diffraction peaks are gradually attenuated with increasing coverage, but have the same positions, indicating the same lattice periodicity as that of the (1×1) -O. The widths of the features do not increase, indicating that the coherence length of the ordered overlayer, estimated to be $>100 \text{ \AA}$, is the same for all coverages. Figure 6(d) shows the ratio of the diffraction features as a function of H₂O coverage. There is a rapid increase up to ~ 0.7 – 1.0 ML of H₂O, followed by a more gradual increase for increasing coverage. At this angle of incidence and azimuth, this behavior is reproducible. Scattering dynamics change with incident conditions: at other angles, the specular feature becomes larger relative to the other diffraction features as H₂O is adsorbed. This is the case for the spectra shown in Fig. 5. Also, as a function of beam flux and hence deposition rate, conditions can be found where the specular intensity as a function of coverage does not monotonically decrease, i.e., the specular signal actually partially recovers after the expected initial decrease over a small coverage range before decreasing again.

These observations are not consistent with diffraction arising only from areas of clean (1×1) -O surrounded by incoherently reflecting islands of H₂O. If this were the case, the ratios of the elastic features would not change. Further, it seems unlikely that such thick overlayers could be deposited without coalescing, or at least leaving increasingly small areas of clean (1×1) -O, which would result in an increase in the widths of the diffraction features.

We feel that the results more likely suggest a novel high-density form of interfacial ice, shown in Fig. 7. Unlike other dense ice structures, which only exist under high pressures,³⁴ this form exists at 10^{-10} Torr. While water is known to dissociate on some metal and metal oxide surfaces, the desorption temperature for water desorbing from (1×1) -O/Rh(111) is close to that of multilayer ice adsorbed on Rh(111). This

indicates that intact molecules of water reside at the (1×1) -O interface. Water desorption due to the reaction of adsorbed OH occurs at much higher temperatures.²⁰ The ice I_h lattice found on Rh(111) is much too open to provide the observed (1×1) He diffraction pattern. One layer of water in this lattice covers only one-third of the Rh atoms. However, the lattice is sufficiently open that it is possible to have two interpenetrating lattices. Distortions of this double lattice occur in known forms of high-pressure ice.³⁴ An undistorted form of this double lattice could be constructed if water molecules adsorbed on the (1×1) -O/Rh(111) form a hydrogen bond at an angle with an adsorbed O, and had the other O-H bond parallel to the surface. Two water orientations would be required, forming the interpenetrating $p(2\times 1)$ -H₂O/ (1×1) -O/Rh(111) structure shown schematically in Fig. 7. Further layers would be deposited by hydrogen bonding to the oxygen of the water molecules in the layer below. This would allow the tetrahedral coordination of hydrogen bonding to persist as in ordinary ice. The 2.74 Å oxygen-oxygen distance of ice I_h would be in close agreement with the 2.69 Å Rh-Rh distance of the surface. Repulsion of the interpenetrating lattices might be expected to expand this bond length and stress the structure. Such stress might be consistent with the observed loss of coherent scattering from thicker overlayers.

CONCLUSIONS

The long-range ordering of H₂O on clean and oxygen pre-dosed Rh(111) has been studied using He atom scattering. On clean Rh(111), or Rh(111) with a small amount of coadsorbed oxygen, the H₂O forms a $(\sqrt{3}\times\sqrt{3})R30^\circ$ structure with a lattice constant of 4.64 ± 0.02 Å, somewhat larger than that of the hexagonal face of ice I_h , 4.50 Å. With our dosing conditions, the surface remains ordered, and with the same lattice constant, up to many layers. The preadsorption of small quantities of oxygen ($0.01\leq\Theta_0\leq 0.05$ ML) improves the long-range order of the H₂O overlayers. The results were much different if larger quantities of oxygen were preadsorbed. When a well-ordered 0.5 ML of oxygen was grown, no long-range order was observed for subsequently deposited H₂O. However, when a full monolayer of oxygen was grown, the adsorbed H₂O exhibited excellent long-range order, but with a (1×1) diffraction pattern. The TPD spectra are indicative of molecular adsorption for the H₂O. *The suggested structure of this water adsorbate is different than that postulated for any other metal or modified metal surface of which we are aware.*

Modifying the Rh(111) surface with a full monolayer of oxygen modifies the bonding arrangement of subsequently adsorbed water. This forms a new high-density form of interfacial ice that is stable at low pressures, unlike the other forms of high-density ice. The existence of this structure opens up the possibility of an ice surface with different chemical activity than previously observed. It also suggests that other molecules, especially those that form hydrogen

bonds, may also exhibit new structures when grown on a high-density oxygen overlayer, creating new pathways for interfacial chemistry.

ACKNOWLEDGMENTS

This work was supported, in part, by the Materials Research Science and Engineering Center Program of the National Science Foundation under Award No. DMR-9808595. Further support from the AFOSR is also gratefully acknowledged.

- ¹D. E. Brown and S. M. George, *J. Phys. Chem.* **100**, 15 460 (1996).
- ²A. Glebov, A. P. Graham, A. Menzel, and J. P. Toennies, *J. Chem. Phys.* **106**, 9382 (1997).
- ³M. Morgenstern, J. Müller, T. Michely, and G. Comsa, *Z. Phys. Chem. (Munich)* **198**, 43 (1997).
- ⁴N. Materer, U. Starke, A. Barbieri, M. A. Van Hove, G. A. Somorjai, G.-J. Kroes, and C. Minot, *Surf. Sci.* **381**, 190 (1997).
- ⁵N. Materer, U. Starke, A. Barbieri, M. A. Van Hove, G. A. Somorjai, G.-J. Kroes, and C. Minot, *J. Phys. Chem.* **99**, 6267 (1995).
- ⁶J. Braun, A. Glebov, A. P. Graham, A. Menzel, and J. P. Toennies, *Phys. Rev. Lett.* **80**, 2638 (1998).
- ⁷P. A. Thiel, *Acc. Chem. Res.* **24**, 31 (1991).
- ⁸P. J. Schmitz, J. A. Polta, S.-L. Chang, and P. A. Thiel, *Surf. Sci.* **186**, 219 (1987).
- ⁹G. Pirug, C. Ritke, and H. P. Bonzel, *Surf. Sci.* **241**, 289 (1991).
- ¹⁰D. L. Doering and T. E. Madey, *Surf. Sci.* **123**, 305 (1982).
- ¹¹P. A. Thiel, R. A. DePaola, and F. M. Hoffmann, *J. Chem. Phys.* **80**, 5326 (1984).
- ¹²G. Held and D. Menzel, *Surf. Sci.* **327**, 301 (1995).
- ¹³G. Held and D. Menzel, *Phys. Rev. Lett.* **74**, 4221 (1995).
- ¹⁴P. A. Thiel, F. M. Hoffmann, and W. H. Weinberg, *J. Chem. Phys.* **75**, 5556 (1981).
- ¹⁵P. A. Thiel, F. M. Hoffmann, and W. H. Weinberg, *Phys. Rev. Lett.* **49**, 501 (1982).
- ¹⁶W. Hoffmann and C. Benndorf, *Surf. Sci.* **377-379**, 681 (1997).
- ¹⁷J. Kiss and F. Solymosi, *Surf. Sci.* **177**, 191 (1986).
- ¹⁸F. T. Wagner and T. E. Moylan, *Surf. Sci.* **191**, 121 (1987).
- ¹⁹J. J. Zinck and W. H. Weinberg, *J. Vac. Sci. Technol. A* **17**, 188 (1980).
- ²⁰P. A. Thiel and T. E. Madey, *Surf. Sci. Rep.* **7**, 211 (1987).
- ²¹K. Röttger, A. Endriss, J. Ihringer, S. Doyle, and W. F. Kuhs, *Acta Crystallogr., Sect. B: Struct. Sci.* **50**, 644 (1994).
- ²²T. E. Madey and F. P. Netzer, *Surf. Sci.* **117**, 549 (1982).
- ²³K. D. Gibson, M. Viste, E. C. Sanchez, and S. J. Sibener, *J. Chem. Phys.* **110**, 2757 (1999).
- ²⁴K. D. Gibson, M. Viste, E. C. Sanchez, and S. J. Sibener, *J. Chem. Phys.* **112**, 2470 (2000).
- ²⁵D. F. Padowitz and S. J. Sibener, *Surf. Sci.* **254**, 125 (1991).
- ²⁶J. I. Colonell, K. D. Gibson, and S. J. Sibener, *J. Chem. Phys.* **103**, 6677 (1995).
- ²⁷B. Poelsema and G. Comsa, *Scattering of Thermal Energy Atoms from Disordered Surfaces* (Springer-Verlag, Berlin, 1989).
- ²⁸F. O. Goodman and H. Y. Wachman, *Dynamics of Gas-Surface Scattering* (Academic, New York, 1976).
- ²⁹A. Zajac, *J. Chem. Phys.* **29**, 1324 (1958).
- ³⁰P. Flubacher, A. J. Leadbetter, and J. A. Morrison, *J. Chem. Phys.* **33**, 1751 (1960).
- ³¹R. S. Smith, C. Huang, E. K. L. Wong, and B. D. Kay, *Surf. Sci.* **367**, L13 (1996).
- ³²H. Witek and V. Buch, *J. Chem. Phys.* **110**, 3168 (1999).
- ³³J. E. Schaff and J. T. Roberts, *J. Phys. Chem.* **100**, 14 151 (1996).
- ³⁴G. A. Jeffrey, *An Introduction to Hydrogen Bonding* (Oxford University Press, New York, 1997), Section 8.3. See, for example, Ice VII in Table 8.2.
- ³⁵G. Held and D. Menzel, *Surf. Sci.* **316**, 92 (1994).